Thermochromism, stability and thermodynamics of cobalt(II) complexes in newly synthesized nitrate based ionic liquid and its photostability

ARTICLE *in* DALTON TRANSACTIONS · AUGUST 2014

Impact Factor: 4.2 · DOI: 10.1039/C4DT01836B

Dalton Transactions

PAPER

View Article Online
View Journal

Cite this: DOI: 10.1039/c4dt01836b

Thermochromism, stability and thermodynamics of cobalt(II) complexes in newly synthesized nitrate based ionic liquid and its photostability

Nemanja Banić, Milan Vraneš, Biljana Abramović, János Csanádi and Slobodan Gadžurić*

In this work a 1-(2-hydroxyethyl)-3-methylimidazolium nitrate ionic liquid, $[HO(CH_2)_2mim]NO_3$, has been synthesized in order to serve as a new thermochromic material upon addition of cobalt(II) ions. Spectrophotometric measurements of a series of cobalt(II) nitrate and cobalt(II) chloride solutions in $[HO(CH_2)_2mim]NO_3$ at 298.15, 308.15, 318.15, 328.15, and 338.15 K, were performed. Based on the recorded spectra, the overall stability constants and thermodynamic parameters for the cobalt(II) associations with chloride and nitrate ions were calculated. The thermodynamic calculations suggest that thermochromism is not observed in the ionic medium due to a small entropy change during the replacement of nitrate with chloride ions in the co-ordination sphere of cobalt(II). The absence of the molecular solvent was also the reason for the lack of thermochromism. Thus, cobalt(II) solutions in $[HO(CH_2)_2mim]NO_3$ and water mixtures were studied as a new and green medium that can be used for the auto-regulation of the light intensity and shade protection. The investigated system with water upon addition of cobalt(II) was found to be a far more efficient and responsive thermochromic medium for all of the studied systems up until now. The structure of $[HO(CH_2)_2mim]NO_3$ was confirmed by both ^1H NMR and IR spectroscopy. Also, the efficiency of different advanced oxidation processes (UV-induced photolysis, UV/H_2O_2 photolysis, heterogeneous photocatalysis using TiO_2 Degussa P25 and TiO_2 with 7.24%, w/w Fe catalysts) for $[HO(CH_2)_2mim]NO_3$ degradation were investigated. The reaction intermediates formed during the photo-oxidation process were identified using LC-ESI-MS/MS and ^1H NMR techniques.

Received 19th June 2014,
Accepted 13th August 2014

DOI: 10.1039/c4dt01836b

www.rsc.org/dalton

Introduction

The possibility to combine thermally responsive chemical processes was studied in this work, in order to attain simultaneous control of temperature and light intensity in agricultural greenhouses and in residential areas. Since sunlight can be directly absorbed by many coloured substances to regenerate heat with achievable temperature below 373.15 K, it is increasingly important to develop new chemical systems that can store and utilize this almost free and readily available solar heat. Research in this area involves the study of new materials and their optical properties upon addition of some thermochromic complex compounds. The thermochromic substance is usually a transition metal, such as cobalt(II) with mixed ligands, undergoing reversible changes to the optical properties in response to a change in temperature, acting thus, as self-regulating shading.[1] Reversibility of the process may provide constant temperature in residential buildings or agricultural greenhouses used for cultivation of some delicate plants in fluctuating climate conditions. In the near future, if incorporated into "smart windows", these materials may cut energy use in buildings, since the windows are significant sources of energy loss.

Research on the ionic association (complex formation) at an early stage have mainly been restricted to aqueous solutions as the reaction media,[2,3] but irreversible water evaporation upon heating is a predictable problem that can shorten the life cycle of the thermochromic devices based on aqueous solutions. Several studies were oriented toward inorganic molten nitrates as a potential medium for thermochromic cobalt(II) halide complex formation,[4,5] but the disadvantage of molten salts was their high melting point, which was the main reason for their low applicability.

By addition of small amounts of a molecular solvent in anhydrous molten salts in order to decrease the melting point, a large number of suitable media in which cobalt(II) halide complexes show thermochromic behaviour were obtained.[6–8]

Faculty of Sciences, Department of Chemistry, Biochemistry and Environmental Protection, University of Novi Sad, Trg Dositeja Obradovića 3, 21000 Novi Sad, Serbia. E-mail: slobodan.gadzuric@dh.uns.ac.rs; Fax: +381 21 454065; Tel: +381 21 4852744

Studies have shown that cobalt(II) thermochromism strongly depends on the amount of added molecular solvent as well as its physical and chemical properties,[9,10] but the reason why this effect occurs in these systems was not successfully explained. Also, it remained an open question whether the thermochromic effect may occur in systems that do not contain molecular solvents, but remain a liquid at temperatures that are low enough for possible application in practice. Therefore, nitrate based ionic liquids were imposed as the ideal answer to this question. Also, the influence of the addition of molecular solvent into room temperature ionic liquids on cobalt(II) thermochromism was not investigated yet, although in our previous papers we already investigated and showed that the presence of a molecular solvent (*e.g.* water, lower amides, dimethylsulfoxide *etc.*) in a mixture with inorganic salts significantly improved cobalt(II) thermochromism.[8–11]

Ionic liquids are excellent solvent candidates due to their unique physical and chemical properties (*e.g.* negligible vapour pressure, low toxicity, non-corrosivity *etc.*). The thermochromic behaviour of chlorido nickel complexes was already investigated in 1-hydroxylalkyl-3-methylimidazolium based ionic liquids.[12] In addition, it is possible to synthesize the required ionic liquid with tunable properties in order to obtain the most suitable solvent. For this reason, ionic liquids are so-called designed solvents. Due to their low toxicity, high conductivity and a significant electrochemical stability, ionic liquids can be used as green solvents and as a replacement of volatile organic solvents in many industrial processes.[13,14]

In this paper, a 1-(2-hydroxyethyl)-3-methylimidazolium nitrate ionic liquid was synthesized and tested as a new ionic material for cobalt(II) thermochromism. This medium contains nitrate as the anion, which is convenient because these ions form octahedral complexes with cobalt(II). Also, nitrate is the weaker ligand compared with chloride, thus the replacement of the ligands is possible upon addition of chloride ions. The polar hydroxyl group as the part of the ionic liquid cation provides better solubility of cobalt(II) salts. Since the complexes of cobalt(II) are coloured, the spectrophotometric method is applied to provide data on the complex structure and coordination of cobalt(II). The influence of the molecular solvent on cobalt(II) thermochromism in ionic medium was also investigated and analysed.

Although the green attributes and tunable properties of ionic liquids have helped scientists develop many green and technologically safer processes, their impact on the environment is still under discussion.[15] For new chemicals, such as ionic liquids, it is very important to evaluate their environmental impact, degradation and stability, as well as complete and safe removal from the environment. Thus, for the first time, the efficiency of different advanced oxidation processes (AOPs) for the removal of the ionic liquid were investigated, including UV-induced photolysis, UV/H_2O_2 photolysis, and also heterogeneous photocatalysis using TiO_2 Degussa P25 (hereafter Degussa P25) and TiO_2 with 7.24%, w/w Fe catalysts, in order to study its stability during exploitation and after use. Recently, these advanced oxidation processes were applied for treating wastewater and degrading organic pollutants such as pesticides, pharmaceuticals, phenols, dyes *etc.*[16–22] An attempt was also made to identify the reaction intermediates formed during the photo-oxidation process, using LC-ESI-MS/MS and ^{1}H NMR techniques.

Results and discussion

Absorption spectra

Absorption spectra of cobalt(II) in both $[HO(CH_2)_2mim]NO_3$ and $[HO(CH_2)_2mim]NO_3{\cdot}3H_2O$ were recorded in the absence of chloride ions at different temperatures: 298.15, 308.15, 318.15, 328.15, and 338.15 K. Spectral properties were examined in this temperature range, because it is also the range of the possible application of the thermochromic material for auto-regulated shading protection. It is clear that the overall molar absorption coefficient increased with increasing temperature (Fig. 1) which is expected for octahedral complexes. These complexes are coloured pale pink.

In Fig. 1 the overall molar absorption coefficient ε, defined as

$$\varepsilon = Al^{-1}c_M{}^{-1}, \quad (1)$$

where A is the absorbance, l the light pathway and c_M is the total cobalt(II) concentration, is plotted against the wavelength.

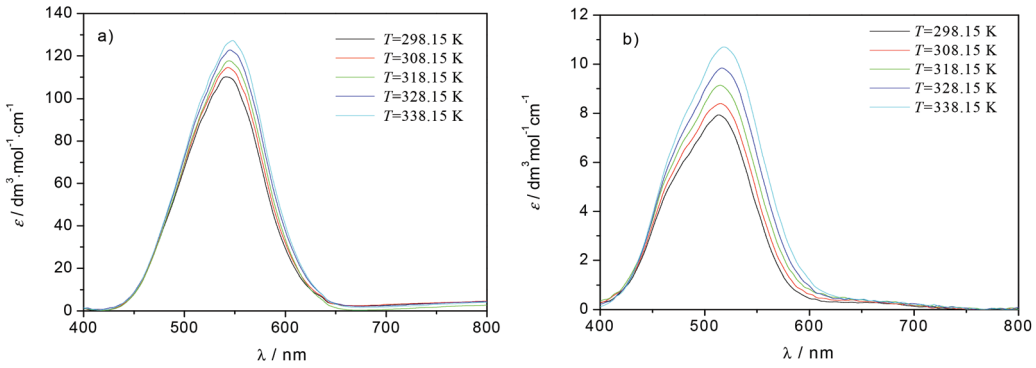

Fig. 1 Absorption spectra of cobalt(II) nitrate in: (a) $[HO(CH_2)_2mim]NO_3$, $m(Co^{2+})$ = 0.01070 mol kg^{-1}, and (b) $[HO(CH_2)_2mim]NO_3{\cdot}3H_2O$, $m(Co^{2+})$ = 0.02960 mol kg^{-1}.

A small shift in the absorption maximum towards lower energies is a consequence of the cobalt(II) ligand field weakening at higher temperatures.[4,5]

Values of the overall molar absorption coefficient in the pure ionic liquid are about ten times higher than in the system with water. This is a consequence of the water co-ordination in the coordination sphere of Co^{2+} ions. In addition, it can be seen that the position of the absorption maximum in the anhydrous system at 544 nm corresponds to the position of the absorption maxima ascribed to the dodecahedral $[Co(NO_3)_4]^{2-}$ complex species obtained in the anhydrous KNO_3–$LiNO_3$ eutectic melt (λ_{max} = 550 nm)[23] and eutectic mixture $0.723CH_3CONH_2$–$0.277NH_4NO_3$ (λ_{max} = 538 nm).[24] In the system of $[HO(CH_2)_2mim]NO_3{\cdot}3H_2O$ the absorption maximum is shifted toward lower wavelengths (approximately at 515 nm) which corresponds to the position of the absorption maximum of octahedral cobalt(II) complexes obtained in the aqueous melt of $Ca(NO_3)_2{\cdot}4H_2O$ (λ_{max} = 512 nm)[25] and diluted aqueous solutions (λ_{max} = 513 nm).[26]

Addition of chloride ions to cobalt(II) nitrate solution caused a replacement of nitrate ions with chloride and formation of new absorbing species:

$$[Co(NO_3)_z]^{2-z} + nCl^- \rightleftarrows [Co(NO_3)_{z-n}Cl_n]^{2-z-n} + nNO_3^- \quad (2)$$

This change is followed by the change in colour from pale pink to dark blue (Fig. 2) and by an appearance of a new absorption band with three maxima, at 634, 669, and 696 nm in both systems.

A large increase in the overall molar absorption coefficient indicates a change from octahedral or dodecahedral to tetrahedral co-ordination (Fig. 3). The tetrahedral maxima occur at slightly higher wavelengths than for the cobalt(II) chloride complexes observed in concentrated aqueous HCl (625, 662, and 692 nm) ascribed to $[CoCl_4]^{2-}$, and the aqueous melt of $Ca(NO_3)_2$–NH_4NO_3–H_2O (626, 662, and 690 nm).[27] The positions of the absorption maxima recorded in $[HO(CH_2)_2mim]NO_3$ have similar values to those observed in anhydrous molten KNO_3–$LiNO_3$ (635, 660, and 690 nm).[4,5]

The influence of temperature on the absorption spectra of cobalt(II) in $[HO(CH_2)_2mim]NO_3$ is presented in Fig. 4. It can be clearly seen that there is no significant change in the intensity of the overall molar absorption coefficients when increasing the temperature, which is a consequence of the absence of the thermochromic effect in pure ionic liquid. Consequently, there is no geometry change of the cobalt(II) from octahedral or dodecahedral to tetrahedral in the studied ionic liquid during the heating or cooling cycles. The reasons for such behaviour (the absence of the cobalt(II) solvolysis in pure ionic liquid and thermodynamic parameters for the complexation reactions) will be discussed later.

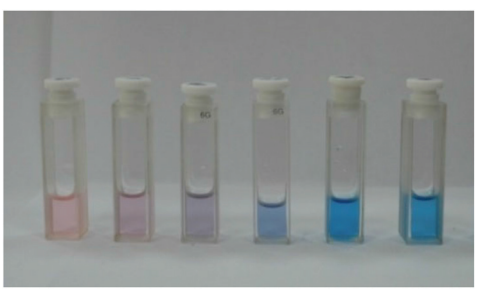

Fig. 2 Colour change of the solutions with an increase of chloride concentration.

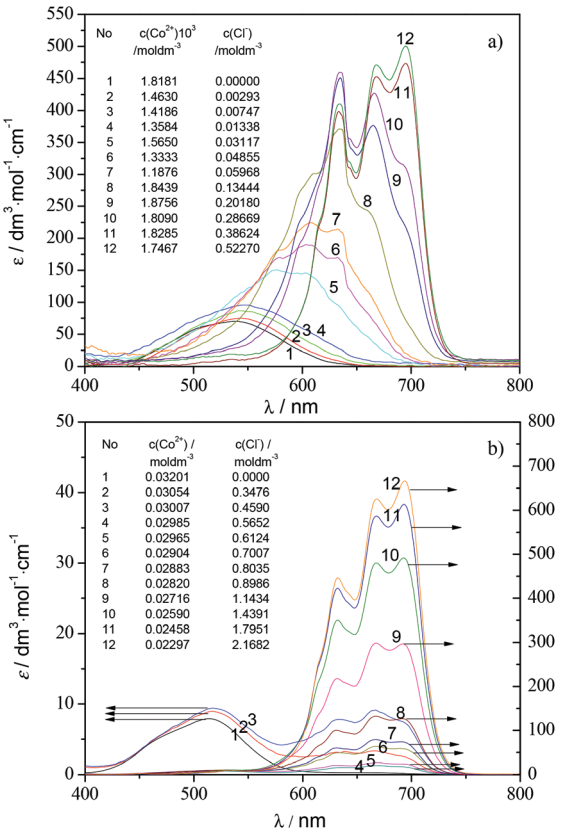

Fig. 3 Variation of cobalt(II) absorption spectra with concentration at 298.15 K in: (a) pure $[HO(CH_2)_2mim]NO_3$, and (b) $[HO(CH_2)_2mim]NO_3{\cdot}3H_2O$.

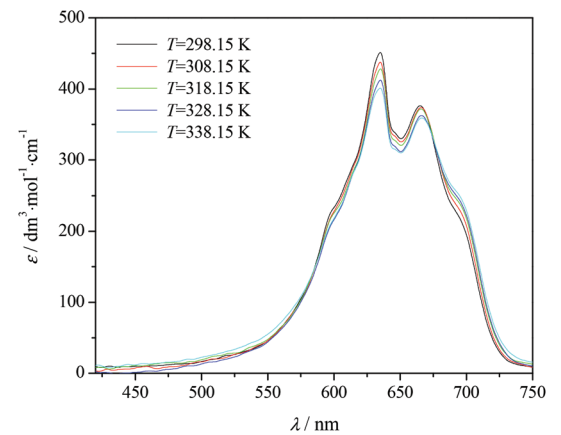

Fig. 4 Absorption spectra of cobalt(II) chloride in $[HO(CH_2)_2mim]NO_3$ at different temperatures; $m(Co^{2+})$ = 0.001440 mol kg^{-1}, $m(Cl^-)$ = 0.15211 mol kg^{-1}.

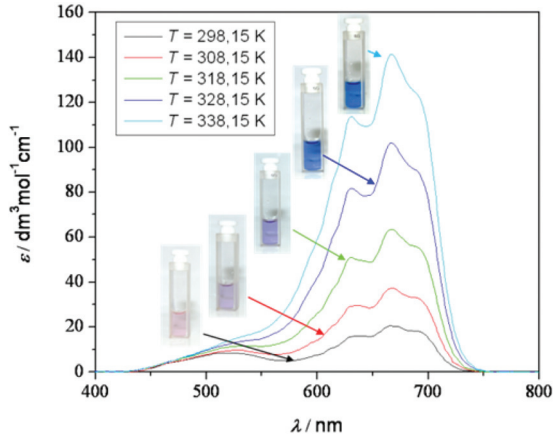

Fig. 5 Absorption spectra of cobalt(II) chloride in $[HO(CH_2)_2mim]NO_3{\cdot}3H_2O$ at different temperatures; $m(Co^{2+})$ = 0.02711 mol kg^{-1}, $m(Cl^-)$ = 0.4448 mol kg^{-1}.

The opposite trend was found upon addition of water as the molecular solvent in the ionic liquid. Here, the increase in temperature leads to a significant increase in the molar absorption coefficients, resulting in a colour change of the solutions (Fig. 5). The same observation was confirmed in our earlier study.[11] However, on the basis of these data it is not possible to conclude why the presence of water was necessary for the existence of thermochromic effect in the system. In order to explain it, stability constants and thermodynamic parameters were calculated on the basis of spectroscopic measurements.

Complex formation equilibrium

Changes in the absorption spectra upon gradual increase in chloride concentration (Fig. 3) are ascribed to complex formation. The complex formation in this mixed ligand system is illustrated by a set of overall equilibrium:

$$Co^{2+} + mNO_3^- + nCl^- \rightleftarrows [Co(NO_3)_mCl_n]^{2-m-n} \quad (3)$$

in the pure ionic liquid, and in the mixture with water:

$$Co^{2+} + pH_2O + qNO_3^- + rCl^- \rightleftarrows [Co(H_2O)_p(NO_3)_qCl_r]^{2-q-r} \quad (4)$$

The overall stability constants are expressed as:

$$\beta_{mn} = [Co(NO_3)_mCl_n{}^{2-m-n}]/[Co^{2+}][NO_3^-]^m[Cl^-]^n \quad (5)$$

$$\beta_{pqr} = [Co(H_2O)_p(NO_3)_qCl_r{}^{2-q-r}]/[Co^{2+}][H_2O]^p[NO_3^-]^q[Cl^-]^r \quad (6)$$

On the basis of cobalt(II) co-ordination by halide ions in other solvents, we assumed that the complexes were mononuclear. For the computation of stability constants the non-linear last-squares programs STAR[28] and HypSpec[29,30] were utilized.

The role of these programs is to determine the number of absorbing species in a chosen wavelength range by factor analysis. From a large number of trials, it was concluded that the following complexes were formed in the case of the pure ionic liquid solution: $[Co(NO_3)_4]^{2-}$, $[Co(NO_3)_3Cl]^{2-}$, $[Co(NO_3)_2Cl_2]^{2-}$, $[Co(NO_3)Cl_3]^{2-}$ and $[CoCl_4]^{2-}$. In the $[HO(CH_2)_2mim]NO_3{\cdot}3H_2O$ system, only three complex species were determined: $[Co(H_2O)_2(NO_3)_4]^{2-}$, $[Co(H_2O)_2(NO_3)_2Cl_2]^{2-}$ and $[CoCl_4]^{2-}$.

The stability constants of these complexes were calculated, together with the molar absorption coefficients of the complexes at each relevant wavelength. The average values of the stability constants calculated by both programs are given in Table 1.

As seen from Table 1, the values of the stability constants in $[HO(CH_2)_2mim]NO_3$ for each complex slightly decrease with temperature, which is not usual behaviour for the cobalt(II) complexes investigated earlier in nitrate melts.[11,27,31] In the case of $[HO(CH_2)_2mim]NO_3{\cdot}3H_2O$, the stability constants increase with temperature as expected.

Thermodynamic parameters

Using the constants from Table 1, the standard thermodynamic functions for the complex formation in $[HO(CH_2)_2mim]NO_3$ and $[HO(CH_2)_2mim]NO_3{\cdot}3H_2O$ were calculated. The standard enthalpy and entropy changes, ΔH^o and ΔS^o, have been estimated from the temperature variation of

$$\Delta G^o = -RT \ln \beta \quad (7)$$

The thermodynamic parameters have been calculated from the formation constants expressed in the molarity scale and obtained values are presented in Table 2. For the conversion of all concentrations expressed as mol kg^{-1}, the density of the investigated solutions was required at different temperatures. The density results are summarized in the Experimental part of the manuscript.

It was found that the formation of all of the complexes is an exothermic process in $[HO(CH_2)_2mim]NO_3$. It is well-known

Table 1 Log(β_{mn}/(mol^{-1} dm^3)^4) for $[Co(NO_3)_mCl_n]^{2-m-n}$ in $[HO(CH_2)_2mim]NO_3$ and log(β_{pqr}/(mol^{-1} dm^3)^4) for $[Co(H_2O)_p(NO_3)_qCl_r]^{2-q-r}$ in $[HO(CH_2)_2mim]NO_3{\cdot}3H_2O$

$[HO(CH_2)_2mim]NO_3$						$[HO(CH_2)_2mim]NO_3{\cdot}3H_2O$		
T/K	$[Co(NO_3)_4]^{2-}$	$[Co(NO_3)_3Cl]^{2-}$	$[Co(NO_3)_2Cl_2]^{2-}$	$[CoNO_3Cl_3]^{2-}$	$[CoCl_4]^{2-}$	$[Co(H_2O)_2(NO_3)_4]^{2-}$	$[Co(H_2O)_2(NO_3)_2Cl_2]^{2-}$	$[CoCl_4]^{2-}$
298.15	2.79 ± 0.05	4.85 ± 0.07	5.70 ± 0.05	7.98 ± 0.20	9.86 ± 0.10	1.09 ± 0.04	1.39 ± 0.08	3.09 ± 0.04
308.15	2.76 ± 0.05	4.70 ± 0.03	5.77 ± 0.21	7.76 ± 0.05	9.61 ± 0.05	1.80 ± 0.03	2.14 ± 0.06	4.00 ± 0.02
318.15	2.69 ± 0.03	4.67 ± 0.02	5.61 ± 0.18	7.55 ± 0.04	9.36 ± 0.02	2.40 ± 0.03	2.79 ± 0.05	4.79 ± 0.02
328.15	2.62 ± 0.05	4.65 ± 0.07	5.45 ± 0.07	7.38 ± 0.09	9.13 ± 0.03	3.10 ± 0.03	3.65 ± 0.05	5.70 ± 0.02
338.15	2.58 ± 0.07	4.62 ± 0.06	5.23 ± 0.10	7.25 ± 0.03	8.95 ± 0.08	3.81 ± 0.03	4.59 ± 0.03	6.58 ± 0.02

Table 2 Standard enthalpy and entropy values for cobalt(II) complex formation in the temperature range from 298.15 to 338.15 K in $[HO(CH_2)_2mim]NO_3$ and $[HO(CH_2)_2mim]NO_3{\cdot}3H_2O$

	$[HO(CH_2)_2mim]NO_3$					$[HO(CH_2)_2mim]NO_3{\cdot}3H_2O$		
	$[Co(NO_3)_4]^{2-}$	$[Co(NO_3)_3Cl]^{2-}$	$[Co(NO_3)_2Cl_2]^{2-}$	$[CoNO_3Cl_3]^{2-}$	$[CoCl_4]^{2-}$	$[Co(H_2O)_2(NO_3)_4]^{2-}$	$[Co(H_2O)_2(NO_3)_2Cl_2]^{2-}$	$[CoCl_4]^{2-}$
ΔH^o/kJ mol^{-1}	−10.9 ± 0.9	−9.8 ± 2.5	−24.6 ± 6.4	−35.4 ± 1.3	−44.5 ± 0.8	130.2 ± 4.2	153.6 ± 9.2	167.7 ± 4.5
ΔS^o/J mol^{-1} K^{-1}	17 ± 3	59 ± 8	29 ± 10	34 ± 4	40 ± 2	457 ± 13	540 ± 29	621 ± 14

that the octahedral–tetrahedral transformation of cobalt(II) is strongly favoured by an increase in temperature or halide concentration or both.[26] Unfortunately, the thermodynamic calculations suggest that octahedral complexes cannot be converted into tetrahedral species in pure ionic liquid. The replacement of the nitrate by the chloride ions is not favoured, since the entropy change is neglected (the total number of species in the system remains the same after complexation). Thus, thermochromism of cobalt(II) in the synthesized ionic liquid was not observed.

Complex formation in the aqueous $[HO(CH_2)_2mim]NO_3{\cdot}3H_2O$ system was found to be endothermic with a prominent entropy change due to the increasing number of species in the reactions. This can be explained by the presence of the water molecules in the co-ordination sphere of dodecahedral cobalt(II) complexes. Since the obtained absorption spectra of tetrahedral $[CoCl_4]^{2-}$ in $[HO(CH_2)_2mim]NO_3{\cdot}3H_2O$ corresponds to the spectra in anhydrous melts, presence of the water molecules in this complex is excluded. Thus, complex formation equilibria in $[HO(CH_2)_2mim]NO_3{\cdot}3H_2O$ can be described by the following equation:

$$[Co(NO_3)_4(H_2O)_2]^{2-} + nCl^- \rightleftarrows [Co(NO_3)_{4-n}Cl_n]^{2-} + nNO_3^- + 2H_2O \quad (8)$$

From all of these observations, it can be concluded that for the existence of cobalt(II) thermochromism in ionic media, the crucial factor is the presence of a small amount of molecular liquid (such as water) which will increase the standard entropy of the complexation reaction and change the geometry of cobalt(II) from octahedral to tetrahedral.

Using the stability constants from Table 1, it was also possible to calculate the resolved species spectra of each complex in both, pure ionic liquid (Fig. 6a) and ionic liquid + water mixture (Fig. 6b). As it can be seen from Fig. 6, resolved spectra for the octahedral complexes formed in the absence of chloride ions, (ε_{40} for $[Co(NO_3)_4]^{2-}$ in $[HO(CH_2)_2mim]NO_3$ and ε_{402} for $[Co(H_2O)_2(NO_3)_4]^{2-}$ in $[HO(CH_2)_2mim]NO_3{\cdot}3H_2O$), are in excellent agreement with the experimental spectra obtained in the solutions without chloride ions (Fig. 1). This also suggests that the calculations, models and conclusions mentioned above in the manuscript are valid and reliable.

The resolved species spectra in pure ionic liquid and $[HO(CH_2)_2mim]NO_3{\cdot}3H_2O$ obtained for $[CoCl_4]^{2-}$ (ε_{04} and ε_{004}) correspond to the tetrahedral co-ordination of cobalt(II) with the characteristic shape of the absorption band, absorption maxima positions and high ε values.

This spectra agrees excellently with those reported for tetrahedral $[CoCl_4]^{2-}$ in solid Cs_2CoCl_4,[32] 12 mol dm^{-3} aqueous HCl,[33] pyridine hydrochloride,[34] and molten alkali chlorides such as eutectic KCl–$AlCl_3$[35] or CsCl.[36]

The resolved spectrum of the mixed chloride–nitrate complex in $[HO(CH_2)_2mim]NO_3{\cdot}3H_2O$ (described in Fig. 6b with ε_{222} overall molar absorption coefficient) showed the most pronounced change in temperature as presented in Fig. 7. It can be concluded that the formation of a mixed complex $[Co(H_2O)_2(NO_3)_2Cl_2]^{2-}$ is the most responsible for thermochromism of cobalt(II) in an ionic liquid and water mixture.

Effects of the type of AOPs

The $[HO(CH_2)_2mim]NO_3$ ionic liquid strongly absorbs UV irradiation over a range of wavelengths, from 200 to 240 nm

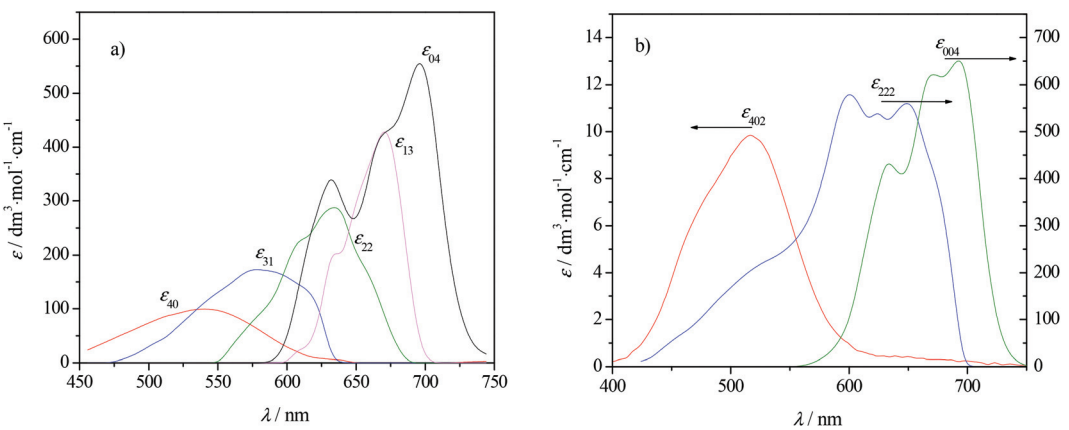

Fig. 6 Resolved species spectra of cobalt(II) complexes in (a) $[HO(CH_2)_2mim]NO_3$ and (b) in $[HO(CH_2)_2mim]NO_3{\cdot}3H_2O$ at 328.15 K.

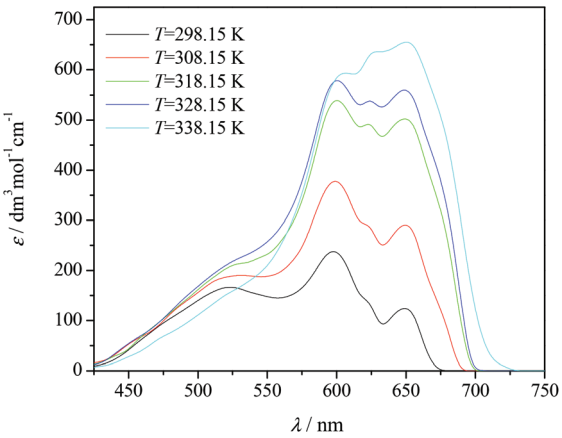

Fig. 7 Resolved species spectra of $[Co(H_2O)_2(NO_3)_2Cl_2]^{2-}$ in $[HO(CH_2)_2mim]NO_3{\cdot}3H_2O$ at different temperatures.

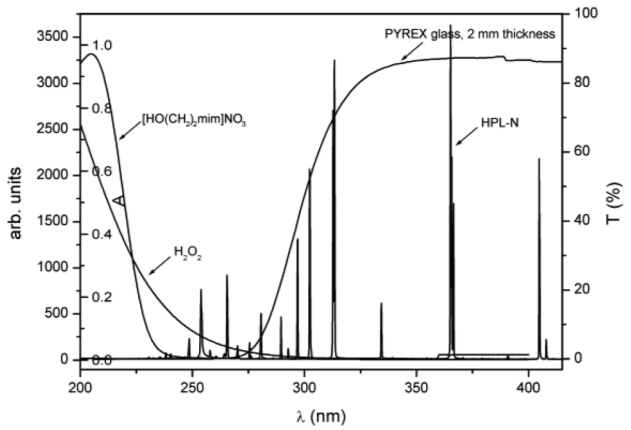

Fig. 8 UV emission spectra of HPL-N lamp (left axis, outer scale) and molar absorption spectrum of $[HO(CH_2)_2mim]NO_3$ (c_0 = 3.8 × 10^{-2} mM) and H_2O_2 (45.3 mM) (left axis, inner scale) and Pyrex glass (right axis).

(Fig. 8), with the maximum absorption band at 210 nm. Hence, only those UV sources with good output below 240 nm can be used for direct photolysis of $[HO(CH_2)_2mim]NO_3$. Since the radiation of a high-pressure mercury lamp below 275 nm can not pass through Pyrex glass, no direct photolysis of $[HO(CH_2)_2mim]NO_3$ could be expected. To investigate the direct photolysis of $[HO(CH_2)_2mim]NO_3$, the first experiments were performed with $[HO(CH_2)_2mim]NO_3$ dissolved in distilled water and at a natural pH of 5.0. After 240 min of irradiation, no significant change in the $[HO(CH_2)_2mim]NO_3$ concentration could be observed (Fig. 9), which is in agreement with the above discussion.

From Fig. 9 (inset) it can be deduced that the decomposition rate in all cases seems to follow a pseudo-first order reaction, and therefore a plot of $\ln(c/c_0)$ *versus* time should give a straight line (the inset of Fig. 9). The rate constants, k, were obtained from least-squares linear regression analysis, all with correlation coefficients greater than 0.98.

Fig. 9 illustrates the efficiency of different AOPs for the degradation of $[HO(CH_2)_2mim]NO_3$. Besides the result of

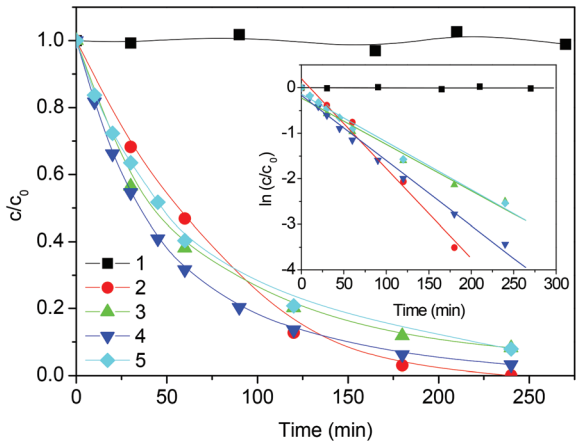

Fig. 9 Degradation kinetics of $[HO(CH_2)_2mim]NO_3$ (c_0 = 0.38 mM) using different procedures: (1) direct photolysis; (2) Degussa P25 (1.67 g l^{-1}); (3) 45 mM H_2O_2 + 70 μl h^{-1} H_2O_2; (4) 7.2Fe/TiO_2 (1.67g l^{-1}) + 45 mM H_2O_2 + 70 μl h^{-1} H_2O_2 at pH 2.80; and (5) 7.2Fe/TiO_2 (1.67g l^{-1}) + 45 mM H_2O_2 + 70 μl h^{-1} H_2O_2 at pH 5.0. The inset shows pseudo-first order kinetics plots.

$[HO(CH_2)_2mim]NO_3$ degradation by direct photolysis, it shows the results of photochemical tests obtained using Degussa P25, H_2O_2, as well as the 7.2Fe/TiO_2/H_2O_2 system. In experiments with H_2O_2, because of its depletion, H_2O_2 was added successively (70 μl each hour during irradiation).

The investigation of the effect of the presence of H_2O_2 showed that indirect photolysis in the presence of H_2O_2 (Table 3) was much more efficient than direct photolysis. These findings indicated that $[HO(CH_2)_2mim]NO_3$ decomposition is enhanced greatly compared to the direct photolysis due to the production of $^{\bullet}OH$ in UV/H_2O_2 process. In addition to this, photodecomposition using Degussa P25 was most efficient, and the complete removal of $[HO(CH_2)_2mim]NO_3$ required only 240 min. The reduced efficiency of indirect photolysis compared to the photocatalytic method with Degussa P25 can be explained by the fact that only radiation with wavelengths less than 300 nm can cause photolysis of hydrogen peroxide.[37] Fig. 8 shows that a relatively small amount of this radiation passes through a Pyrex glass. On the other hand, from the absorption spectrum of Degussa P25[37] it can be concluded that all radiation that passes through the Pyrex glass was used, which leads to an increased degradation efficiency.

Table 3 Rate constants of $[HO(CH_2)_2mim]NO_3$ degradation by UV, UV/TiO_2, UV/H_2O_2, UV/7.2Fe/TiO_2/H_2O_2 processes (c_0 = 0.38 mM)

Process	Initial pH	Rate constant, $(k \times 10^2)/min^{-1}$	Removal[a]/ %
Photolysis	5.0	—	—
Degussa P25	5.0	1.98	100
45 mM H_2O_2 + 70 μl h^{-1} H_2O_2	5.0	1.02	91.8
7.2Fe/TiO_2 + 45 mM H_2O_2 + 70 μl h^{-1} H_2O_2	5.0	1.05	92.1
7.2Fe/TiO_2 + 45 mM H_2O_2 + 70 μl h^{-1} H_2O_2	2.8	1.43	96.8

[a] Removal percentage at 240 min.

The 7.2Fe/TiO_2/H_2O_2 system was used to study the efficiency of heterogeneous photo-Fenton oxidation. For this system photodegradation experiments were conducted at pH 5.0 and 2.8,[17] and as can be seen from Table 3 this change only altered the removal efficiency by 4.7%.

As can be seen from Table 3, the degradation efficiencies of four different processes increases in the following order: UV < UV/H_2O_2 < UV/7.2Fe/TiO_2/H_2O_2 < UV/TiO_2. It should be noted that for the last three photochemical processes, the degradation efficiency after 240 min varies by only 8%, and from the standpoint of environmental protection, cost of chemicals and in conjunction with artificial sources of radiation the most applicable method would be the UV/H_2O_2 process.

Intermediates of photodegradation

Identification of the intermediates was also carried out using ^{1}H NMR (Fig. 10). The standard proton spectrum recorded for [HO(CH_2)$_2$mim]NO_3 in D_2O before irradiation contained the following significant signals [δ_H (ppm)]: 8.72 (*s*, 1H, H-2), 7.45 (*d*, 2H, $J_{4,5}$ = 14 Hz, H-4 and H-5), 4.28 (*m*, 2H, OCH_2), 3.89 (*m*, 2H, NCH_2), and 3.87 (*s*, 3H, NCH_3)].

After 120 minutes of photodegradation in the NMR spectrum three new signals were identified, at 2.99, 2.73 and 2.56 ppm. The intensities of these signals were increased as degradation of the starting [HO(CH_2)$_2$mim]NO_3 moiety progressed. Also, after the same amount of degradation, in the NMR spectrum a signal was observed at 8.92 ppm which originates from the changed aromatic structure. The signal intensity of this intermediate (8.92 ppm) showed a slower increase during photodegradation. During the entire period of photodegradation, in the aromatic region the existence of another intermediate was observed (signal at 8.87 ppm) with very low actual concentration. In addition, after 240 minutes of degradation the new signal was observed at 3.77 ppm. In the next five hours of degradation, the intensity of this signal increased, and then decreased until the end of the experiment.

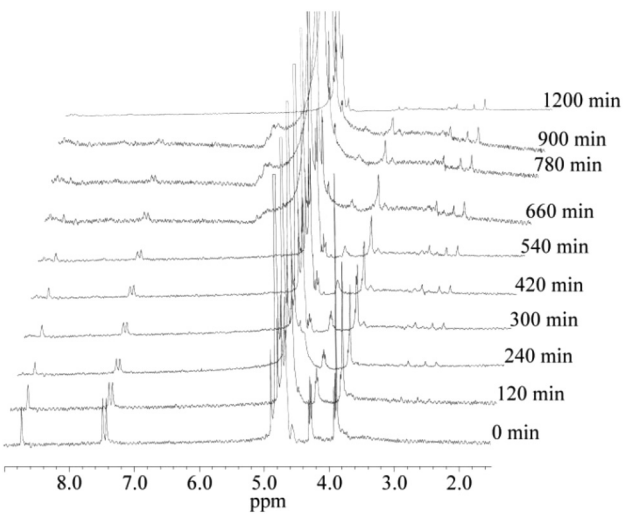

Fig. 10 Temporal ^{1}H NMR spectral profiles during the photodecomposition of [HO(CH_2)$_2$mim]NO_3 in a D_2O solution (c_0 = 3.8 mM) in the presence of Degussa P25 (1.67 g l^{-1}).

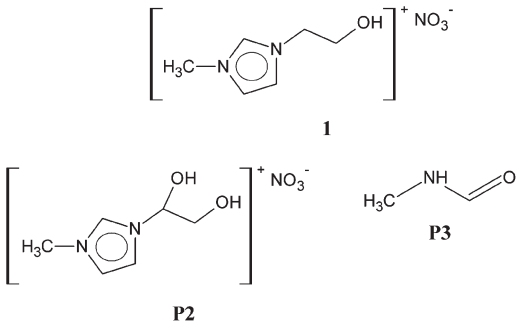

Fig. 11 Structure of the studied [HO(CH_2)$_2$mim]NO_3 (**1**) and proposed structures for photodegradation products (**P2**) and (**P3**) in the presence of Degussa P25.

The existence of *N*-methylformamide (**P3**) in Fig. 11, as the intermediate formed during the photocatalytic degradation was confirmed by adding an authentic internal standard of *N*-methylformamide and overlapping its signals with those obtained during the photodegradation [δ_H (ppm)]: [2.71 (*s*, NCH_3), 7.97 (*s*, COH)]. Based on the kinetic curves and the corresponding absorption spectra of the intermediates obtained from the HPLC–DAD method, the existence of this intermediate is also established in the experiment of indirect photolysis (Fig. 9). The LC–ESI-MS/MS technique identified [HO(CH_2)$_2$mim]NO_3 (**1**) and **P2** (Fig. 11) based on their MS/MS fragmentation data (Table 4).

P2 (likely 1-(1,2-dihydroxyethyl)-3-methylimidazolium nitrate) represents a compound with M_{mi} = 142, which is 16 units higher than the molecular mass of [HO(CH_2)$_2$mim]NO_3 and that indicates the addition of the hydroxyl group. The intermediate **P2** fragmentation starts with water loss ($\Delta m/z$ = 18) from a secondary alcohol. The formed enol isomerizes into an aldehyde, which loses CO ($\Delta m/z$ = 28) yielding the 1,3-dimethylimidazolium cation. A parallel reaction also forms the methylimidazolium cation (m/z = 83) by loss of a ketene ($\Delta m/z$ = 42) from an aldehyde. The final fragmentation product, the methylazirenium ion (m/z = 56) is formed by HCN loss ($\Delta m/z$ = 27) accompanied by ring contraction.

Table 4 MS/MS fragmentation data for [HO(CH_2)$_2$mim]NO_3 (**1**) and its intermediate obtained in positive ion mode

Peak label	M_{mi}/ g mol^{-1}	Precursor ion m/z	V_{col}/V	Product ions m/z (relative abundance)
1	126	127	0	127 (100)
			10	127 (100), 83 (58)
			20	127 (11), 83 (100)
			30	95 (6), 83 (100), 56 (16)
P2	142	143	0	143 (100), 125 (14)
			10	143 (30), 125 (100), 97 (7)
			20	125 (100), 97 (43), 96 (34), 95 (26), 83 (11), 56 (12)
			30	125 (13), 97 (22), 96 (52), 95 (100), 83 (13), 56 (20)

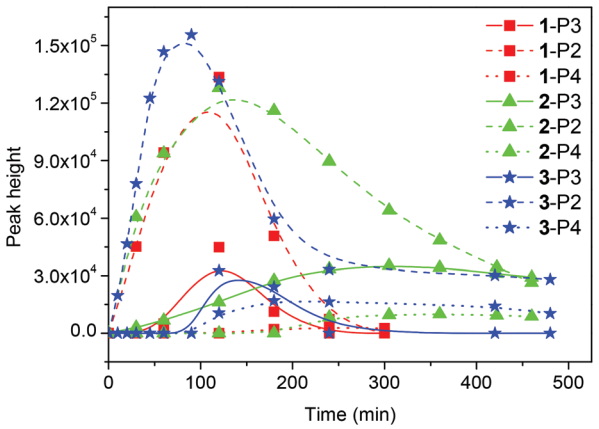

Fig. 12 Kinetics of intermediate formation during photodegradation of $[HO(CH_2)_2mim]NO_3$ (c_0 = 0.38 mM) by different AOPs: (**1**) Degussa P25 (1.67 g l^{-1}); (**2**) 45 mM H_2O_2 and 70 μl h^{-1} H_2O_2; (**3**) 7.2Fe/TiO_2 (1.67g l^{-1}) and 45 mM H_2O_2 and 70 μl h^{-1} H_2O_2 at pH 2.80.

Based on the obtained data (Fig. 12) it can be concluded that the induced photolytic with H_2O_2 and photocatalytic degradation follow the same reaction mechanism. The methods used cannot determine the structure of **P4**, but it is supposed that the magnification nonpolarity (HPLC-DAD results) was probably due to oxidation of the hydroxyl groups of **P2** and introducing a carbonyl group.

Experimental part

Chemicals and solutions

All of the chemicals used were pro analysis products. For the synthesis of the ionic liquid, 2-chloro-1-ethanol (Fluka), *N*-methylimidazole (Sigma-Aldrich), ethyl acetate (Backer) and silver nitrate (Poch) were used.

The synthetic path of 1-(2-hydroxyethyl)-3-methylimidazolium nitrate is presented in Fig. 13. A 250 cm^3 three-neck round-bottom flask was filled with 2-chloro-1-ethanol (88 cm^3, 1.30 mol), freshly distilled *N*-methylimidazole (94 cm^3, 1.17 mol) and 50 cm^3 of ethyl acetate. The mixture was stirred and heated under reflux for one week at 352 K. Yellow crystals were obtained after cooling. The solid was re-crystallized from

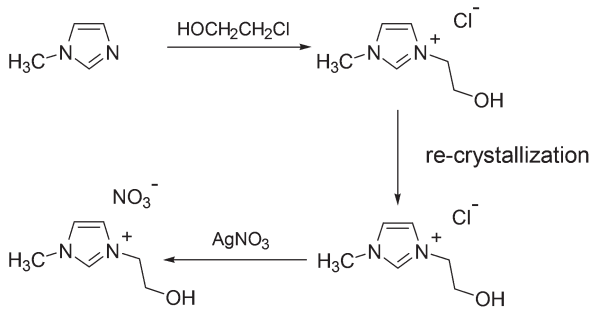

Fig. 13 Synthetic path of 1-(2-hydroxyethyl)-3-methylimidazolium nitrate.

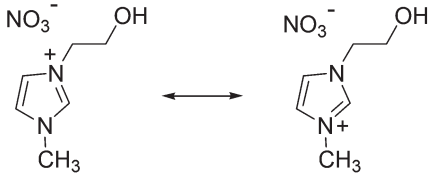

Fig. 14 The resonant structures of 1-(2-hydroxyethyl)-3-methylimidazolium nitrate.

dry ethanol four times. The purity of the obtained white crystals was checked by potentiometric titration of the chloride ions (ω(Cl) = 0.9801). Then, a calculated amount of the crystals (69.2 g, 0.4259 mol) was mixed with $AgNO_3$ (74.0 g, 0.4354 mol) and 60 cm^3 of water. The mixture was stirred in a round-bottom flask for 120 minutes. The resulting white precipitate (silver chloride) was removed and the obtained liquid is purified using activated charcoal. A clear colourless liquid was obtained. The yield of the product was 95%. (The amount of silver and chloride ions in the product was determined by potentiometric titration.) In order to remove water and other volatile organic compounds from the sample, the ionic liquid was heated for 72 h at 323.15 K under vacuum. Then, it was conditioned under a nitrogen atmosphere, which was selected because of its low solubility in the investigated ionic liquids. After drying, the water content in the IL was found to be less than 10^{-4}%.

The ^{13}C and ^{1}H NMR spectra of the ionic liquid were recorded on a Bruker AC-250 spectrometer. ^{1}H NMR (D_2O): δ 3.92 (*s*, 3 H); 3.92 (*t*, 2 H); 4.41 (*t*, 2 H, J = 4.8 Hz); 7.55 and 7.60 (2 × *s*, 2 H); 8.85 (*s*, 1 H). ^{13}C NMR (D_2O): δ 38.12 (*q*, CH_3); 54.09 (*t*, CH_2CH_2OH); 62.36 (*t*, CH_2CH_2OH); 124.92 and 126.02 (2 × *dd*, C-4 and C-5); 139.04 (*d*, C-2). Two resonant structures of the investigated ionic liquid are presented in Fig. 14.

For additional characterization, the IR spectra of the ionic liquids were recorded. The observed peak at 1344 cm^{-1} indicates the presence of nitrate ions, while the peak appeared at 3394 cm^{-1} indicates the existence of a hydroxyl group in the ionic liquid.

Density

A vibrating tube densimeter, Rudolph Research Analytical DDM 2911, was used for density measurements. The accuracy and precision of the densimeter were ±0.00001 g cm^{-3}. The instrument was automatically thermostated (Peltier-type) within ±0.02 K and was calibrated at the atmospheric pressure before each series of measurements. The calibration was performed using ambient air and bidistilled ultra pure water. The density of the samples was measured in the temperature range from 283.15 K up to 353.15 K at different chloride concentration. The density dependence on temperature (T in K) and chloride concentration (m in mol kg^{-1}) was a linear function and may be summarized by the following relation:

$$d = 1.35371 - 8.297 \times 10^{-4}T + (0.00625 + 4,58 \times 10^{-5}T)m(Cl^-) \quad (9)$$

Vis-spectroscopy

The stock solution of cobalt(II) nitrate in ionic liquid was prepared by measuring the appropriate amounts of $Co(NO_3)_2{\cdot}6H_2O$ and $[HO(CH_2)_2mim]NO_3$. The solution was heated to remove the water from the system, which has been previously added as cobalt(II) nitrate hexahydrate. The series of 11 solutions with different cobalt(II)/chloride ratios (from 2 to 300) in pure ionic liquid were prepared for the spectrophotometric measurements. For the measurements of the cobalt(II) absorption spectra in $[HO(CH_2)_2mim]NO_3{\cdot}3H_2O$, the appropriate amounts of ionic liquid, $Co(NO_3)_2{\cdot}6H_2O$ and water were measured. The series of 14 solutions with different cobalt(II)/chloride ratios (from 0 to 95) in this solvent were prepared and recorded spectrophotometrically.

The absorption spectra of the solutions with variable chloride and cobalt(II) concentration were recorded in the wavelength range 400–800 nm on a Secomam Anthelie Advanced 2 spectrophotometer with thermostated cell compartments at 298.15, 308.15, 318.15, 328.15 and 338.15 K. The temperature was kept constant, ±0.1 K.

Photostability of 1-(2-hydroxyethyl)-3-methylimidazolium nitrate

The concentration of the 1-(2-hydroxyethyl)-3-methyl-imidazolium nitrate stock solution used in photodegradation experiments was 0.38 mM and 3.8 mM. 30% H_2O_2, 99.8% acetonitrile (ACN, HPLC gradient grade), and 99% *N*-methylformamide were purchased from Sigma-Aldrich; 85% H_3PO_4 was a product Lachema (Neratovice, Czech Republic); NaOH was a product of Zorka Pharm (Šabac, Serbia), and H_2SO_4 was purchased from Merck. All solutions were made using doubly distilled water, except for the ^{1}H NMR measurements where 99.9% D_2O purchased from Sigma-Aldrich was used as solvent.

Fe/TiO_2 with 7.24% of Fe (w/w, denoted as 7.2Fe/TiO_2)[15] and Degussa P25 (75% anatase and 25% rutile form, surface area of 50 m^2 g^{-1}, and average particle size about 20 nm, according to the producer's specification), were used as photocatalysts.

Photodegradation procedure

A typical photocatalytic experiment was carried out in a batch reactor made of Pyrex glass (total volume of *ca.* 100 cm^3, solution depth 46 mm). A Philips HPL-N 125 W high-pressure mercury lamp (λ > 290 nm) was used as the UV source. It has emission bands in the UV region at 304, 314, 335 and 366 nm, with a maximum emission at 366 nm. The radiation intensity was 3.57 mW cm^{-2}.

The experiments were carried out using 30 cm^3 $[HO(CH_2)_2mim]NO_3$ solution containing 1.67 g l^{-1} of catalyst and/or 45 mM H_2O_2 with the successive addition of H_2O_2 (70 μl each hour during the radiation) (except for the study of direct photolysis). In the case of Degussa P25 as the catalyst, H_2O_2 was absent. All experiments were performed at the natural pH (~5.0), except when studying the influence of the pH on the 7.2Fe/TiO_2 catalyst. The pH was adjusted by adding a solution of H_2SO_4 or NaOH. The suspension was stirred continuously in the dark for 15 min prior to turning on the UV lamp so as to ensure equilibrium adsorption of $[HO(CH_2)_2mim]NO_3$ on the photocatalyst. Oxygen (99.99% purity) was continuously fed to the bottom of the reactor at a constant flow rate of 5 cm^3 min^{-1}. Apart from oxygen bubbling, the solution was homogenized with the aid of a stirring bar, to ensure completely mixed batch conditions. The control experiments carried out under O_2 flow by stopping the irradiation showed that there were no losses of volatile compounds during the degradation. The temperature of the reaction solution was maintained at 298 ± 0.5 K throughout the experiment using a water circulation system.

Analytical procedure

For the kinetic studies of $[HO(CH_2)_2mim]NO_3$ (0.38 mM) removal and its photodegradation intermediates by liquid chromatography-diode array detection (HPLC-DAD), 0.5 cm^3 aliquots of the reaction mixture were sampled at the beginning of the experiment and at various time intervals, followed by filtration through a Millipore (Millex-GV, 0.22 μm) membrane filter (in the presence of photocatalyst). The absence of adsorption of the ionic liquid onto the filters was confirmed by a preliminary test. A Shimadzu UFLC liquid chromatograph equipped with UV-vis diode array detection and a Zorbax Eclypse XDB-C18 (150 mm × 4.6 mm i.d., particle size 5 μm) column were used. The injection volume was 20 μl. Column temperature was held at 298.15 K, the eluent was a mixed solution of 0.1% H_3PO_4–ACN (6 : 4, v/v), pH 2.56, and the total flow rate was 0.8 cm^3 min^{-1}. The ionic liquid elution was monitored at 210 nm (absorption maximum for ionic liquid), with a retention time of 1.54 min.

Absorbance spectra were recorded on a double-beam T80+ UV-vis Spectrometer (UK), at a fixed slit width (2 nm), using a 1 cm quartz cell and computer-loaded UV Win 5 data software. The UV energy flux was measured using a Delta Ohm HD 2102.2 (Padova, Italy) radiometer that was fitted with the LP 471 UVA sensor (spectral range 315–400 nm).

The ^{1}H NMR spectra of $[HO(CH_2)_2mim]NO_3$–D_2O solution (3.8 mM, sample volume 1.0 cm^3) during illumination in the presence of Degussa P25 particles were recorded on a Bruker AC-250 spectrometer. Filtration was carried out to separate the TiO_2 particles as previously described. Experimental conditions: temperature of samples 296 K, data points 16 K, time domain 16 K, receiver gain 10, pulse width 3.0 μs, acquisition time 2.736 s, spectral width 3000 Hz, and line broadening 0.2. The numbers of scans was 265.

For the LC-ESI-MS/MS evaluation of intermediates 3.8 mM of $[HO(CH_2)_2mim]NO_3$ was prepared. Filtration was carried out to separate the Degussa P25 particles as previously described. Then, a 20 μl sample was injected and analyzed on an Agilent Technologies 1200 series LC with Agilent Technologies 6410A series electrospray ionization triple-quadrupole MS/MS, using Agilent Technologies Zorbax XDB-C18 column (50 mm × 4.6 mm i.d., particle size 1.8 μm, 313 K). The mobile phase (flow rate 1 cm^3 min^{-1}) consisted of 0.1% aqueous formic acid

and ACN (gradient: 0 min 30% ACN, 1.5 min 40.5%, post time 0.5 min). Analytes were ionized using the electrospray ion source, with nitrogen as the drying gas (temperature 623 K, flow 10 dm^3 min^{-1}) and nebulizer gas (45310.26 kPa), and a capillary voltage of 4.0 kV. High-purity nitrogen was used as the collision gas. Full scan mode (*m*/*z* range 50–500, scan time 100 ms, fragmentor voltage 100 V), using both polarities, was adopted to examine isotopic peaks distribution and obtain structural information. To identify the detected compounds, product ion scan analysis (MS^2 experiment) was used, with $[M + H]^+$ ions as precursors, and collision energies in 10–30 V interval (10 V increments).

Conclusions

Ionic liquid 1-(2-hydroxyethyl)-3-methylimidazolium nitrate was synthesized in this work. The structure was confirmed by both ^1H NMR and IR spectroscopy. The density of this liquid was measured in the temperature range from 283.15 K to 353.15 K. The spectrophotometric measurements of cobalt(II) nitrate and cobalt(II) chloride series solutions in $[HO(CH_2)_2mim]NO_3$ and $[HO(CH_2)_2mim]NO_3{\cdot}3H_2O$ at 298.15, 308.15, 318.15, 328.15, and 338.15 K, were performed. According to the spectrophotometric measurements and calculations of the stability constants and thermodynamic parameters, it was concluded that pure ionic liquid due to the absence of cobalt(II) solvolysis and unfavourable entropy values for the complexation reaction, could not be used as a suitable medium for cobalt(II) thermochromism. Addition of a small amount of molecular solvent (water) increases the entropy of the system and pronounces thermochromism of cobalt(II) in an ionic liquid and water mixture. Also, the photostability of $[HO(CH_2)_2mim]NO_3$ was examined for the first time by applying four different AOPs: UV, UV/H_2O_2, UV/7.2Fe/TiO_2/H_2O_2 and UV/TiO_2 Degussa P25. It was observed that indirect photolysis in the presence of H_2O_2 was much more efficient than direct photolysis. By applying photocatalyst Degussa P25 and 7.2Fe/TiO_2/H_2O_2 after 240 minutes of UV irradiation, complete decomposition of the ionic liquids was achieved. For the 7.2Fe/TiO_2/H_2O_2 system a change in pH value from 5.0 to 2.8 had no effect on the efficiency of $[HO(CH_2)_2mim]NO_3$ degradation. It was also found that the decomposition rate of $[HO(CH_2)_2mim]NO_3$ for all applied AOPs followed a pseudo-first order reaction. For the studied AOPs the same degradation products were found, which points to the same mechanism of degradation.

Acknowledgements

This work was financially supported by the Ministry of Education, Science and Technological Development of Republic of Serbia under project contracts ON172012, ON172042 and The Provincial Secretariat for Science and Technological Development of APV.

Notes and references

1 M. Santamouris, C. A. Balaras, E. Descalaki and M. Vallindras, *Sol. Energy*, 1994, **53**, 411.
2 P. Pan and N. J. Susak, *Geochim. Cosmochim. Acta*, 1989, **53**, 327.
3 L. H. Skibsted and J. Bjerrum, *Acta Chem. Scand.*, 1978, **32**, 429.
4 I. V. Tananaev and R. F. Dzurinskii, *Dokl. Akad. Nauk SSSR*, 1960, **134**, 1374.
5 I. V. Tananaev and R. F. Dzurinskii, *Dokl. Akad. Nauk SSSR*, 1960, **135**, 1394.
6 D. H. Kerridge, R. Nikolić and D. Stojić, *J. Chem. Soc., Dalton Trans.*, 1986, 1663.
7 J. Savović, R. Nikolić and D. Veselinović, *J. Solution Chem.*, 2004, **33**, 287.
8 B. Matijević, I. Zsigrai, M. Vraneš and S. Gadžurić, *J. Mol. Liq.*, 2010, **154**, 82.
9 M. Vraneš, S. Gadžurić, S. Dožić and I. Zsigrai, *J. Chem. Eng. Data*, 2010, **55**, 2000.
10 M. Vraneš, S. Gadžurić, I. Zsigrai and S. Dožić, *J. Mol. Liq.*, 2010, **152**, 34.
11 S. Gadžurić, M. Vraneš and S. Dožić, *Sol. Energy Mater. Sol. Cells*, 2012, **105**, 309.
12 X. Wei, L. Yu, D. Wang, X. Jin and G. Z. Chen, *Green Chem.*, 2008, **10**, 296.
13 M. Koel, *Ionic Liquids in Chemical Analysis*, Taylor & Francis Group, CRC, New York, 2009.
14 A. Berthod and B. S. Carda, *Anal. Bioanal. Chem.*, 2004, **380**, 168.
15 D. Adam, *Nature*, 2000, **407**, 938.
16 B. F. Abramović, N. D. Banić and D. V. Šojić, *Chemosphere*, 2010, **81**, 114.
17 N. Banić, B. Abramović, J. Krstić, D. Šojić, D. Lončarević, Z. Cherkezova-Zheleva and V. Guzsvány, *Appl. Catal., B*, 2011, **107**, 363.
18 D. Šojić, V. Despotović, D. Orčić, E. Szabó, E. Arany, S. Armaković, E. Illés, K. Gajda-Schrantz, A. Dombi, T. Alapi, E. Sajben-Nagy, A. Palágyi, Cs. Vágvölgyi, L. Manczinger, L. Bjelica and B. Abramović, *J. Hydrol.*, 2012, **314**, 472–473C.
19 S. Ahmed, M. G. Rasul, W. N. Martens, R. Brown and M. A. Hashib, *Desalination*, 2010, **261**, 3.
20 A. Y. C. Tong, R. Braund, D. S. Warren and B. M. Peake, *Cent. Eur. J. Chem.*, 2012, **10**, 989.
21 M. Pera-Titus, V. García-Molina, M. A. Baños, J. Giménez and S. Esplugas, *Appl. Catal., B*, 2004, **47**, 219.
22 P. R. Gogate and A. B. Pandit, *Adv. Environ. Res.*, 2004, **8**, 553.
23 S. Hemmingsson and B. Holmberg, *Inorg. Chem.*, 1980, **19**, 2242.
24 I. Zsigrai, S. Gadžurić and B. Matijević, *Z. Naturforsch, A: Phys. Sci.*, 2005, **60**, 201.
25 I. Zsigrai, S. Gadžurić, R. Nikolić and L. Nagy, *Z. Naturforsch., A: Phys. Sci.*, 2004, **59**, 602.
26 F. A. Cotton and G. Wilkinson, *Advanced Inorganic Chemistry*, John Wiley and Sons, New York, 1988, vol. 3.

27 M. Vraneš, S. Gadžurić and I. Zsigrai, *J. Mol. Liq.*, 2007, **135**, 135.
28 J. L. Beltran, R. Codony and M. D. Prat, *Anal. Chim. Acta*, 1993, **276**, 441.
29 P. Gans, A. Sabatini and A. Vacca, *Talanta*, 1996, **43**, 1739.
30 P. Gans, A. Sabatini and A. Vacca, *Ann. Chim.*, 1999, **89**, 45.
31 M. Vraneš, S. Gadžurić and I. Zsigrai, *J. Mol. Liq.*, 2009, **145**, 14.
32 H. W. Smith and W. J. Stratton, *Inorg. Chem.*, 1977, **16**, 1640.
33 C. J. Balhausen and C. K. Jørgensen, *Acta Chem. Scand.*, 1955, **9**, 397.
34 D. M. Gruen, *J. Inorg. Nucl. Chem.*, 1957, **4**, 74.
35 H. A. Øye and D. M. Gruen, *Inorg. Chem.*, 1965, **4**, 1173.
36 C. A. Angell and D. M. Gruen, *J. Inorg. Nucl. Chem.*, 1967, **29**, 2243.
37 S. Malato, P. Fernández-Ibáñez, M. I. Maldonado, J. Blanco and W. Gernjak, *Catal. Today*, 2009, **147**, 1.